JACS
JOURNAL OF THE AMERICAN CHEMICAL SOCIETY
pubs.acs.org/JACS

Article

Chemoproteomics of Marine Natural Product Naamidine J Unveils CSE1L as a Therapeutic Target in Acute Lung Injury

Cheng-Long Gao,[¶] Jin-Qian Song,[¶] Ze-Nan Yang,[¶] Haojie Wang, Xin-Yuan Wu, Changwei Shao, Hong-Xia Dai, Kaixian Chen, Yue-Wei Guo,* Tao Pang,* and Xu-Wen Li*

Cite This: J. Am. Chem. Soc. 2024, 146, 28384−28397

Read Online

ACCESS | Metrics & More | Article Recommendations | Supporting Information

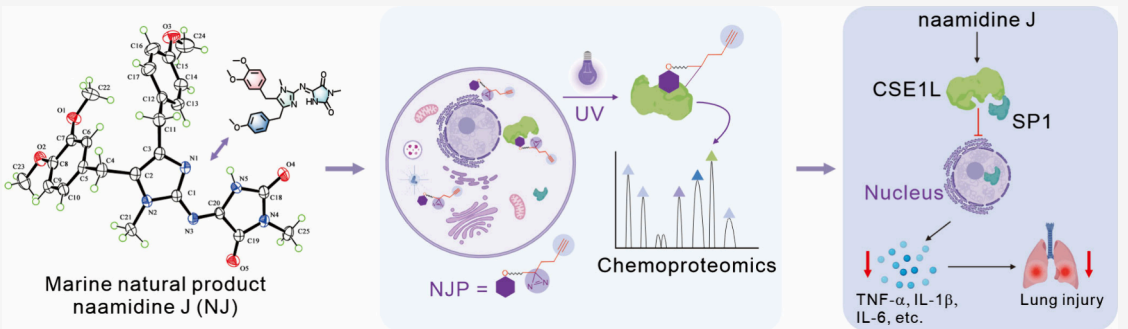

ABSTRACT: Acute lung injury is a devastating illness characterized by severe inflammation mediated by aberrant activation of macrophages, resulting in significant morbidity and mortality, highlighting the urgent need for novel pharmacological targets and drug candidates. In this study, we identified a novel target for regulating inflammation in macrophages and acute lung injury via chemical proteomics and genetics based on a marine alkaloid, naamidine J (NJ). The structures of NJ-related naamidine alkaloids were first confirmed or revised by a combination of quantum chemical calculations and X-ray diffraction analysis. NJ was found as a potential anti-inflammatory agent by screening our compound library, and CSE1L was identified by chemoproteomics as a main cellular target of NJ to inhibit inflammation in macrophages and protect against acute lung injury. Mechanistically, we demonstrated that NJ directly interacted with CSE1L on the sites of His745 and Phe903 and then inhibited the nuclear translocation and transcriptional activity of transcription factor SP1, thereby suppressing inflammation in macrophages and ameliorating acute lung injury. Taken together, these findings have uncovered a novel pharmacological target for the treatment of acute lung injury and have also provided a potential druggable pocket of CSE1L and a lead compound or an available chemical tool from marine sources for investigating CSE1L function and developing novel drug candidates against acute lung injury.

INTRODUCTION

Alveolar macrophages are the sentinel cells of the alveolar space and are the first defense line of the innate immune system in lung tissue, endowed with cytosolic and membrane receptors allowing for a "high-alert" state regarding any invading pathogens,[1−3] and play a vital role in maintaining homeostasis, fending off pathogens, and controlling lung inflammation.[3] During inflammatory disease of acute lung injury, overactivated macrophages and neutrophils recruited by macrophages produce abundant pro-inflammatory factors resulting in cellular cytokine storm, which leads to severe cell death and lung tissue damage.[3−7] In addition, macrophages also repair damaged tissues by altering the state of macrophage polarization or by interacting with other cells through the secretion of various cytokines and chemical mediators.[7] The central and crucial role of macrophages in acute lung injury leads to macrophages being attractive targets for therapeutic interventions. Besides, increasing evidence has shown that intervention of uncontrolled and severe inflammatory response is one of the most effective therapies for the treatment of inflammatory disease, such as acute lung injury.[3,6,8,9] However, until now, there are still no drugs to treat acute lung injury approved by the FDA, and it is urgent to discover novel targets and candidates for the therapy of acute lung injury associated with macrophage-mediated inflammation.

Chromosome segregation 1-Like Protein (CSE1L), also known as exportin-2 (XPO2), is a nuclear transport (export) factor. CSE1L and importin α coregulate the nuclear to cytoplasmic recycling of proteins (histone deacetylase) and nucleic acids (mRNA and circular RNA).[10−13] A large amount

Received: July 17, 2024
Revised: September 12, 2024
Accepted: September 16, 2024
Published: September 26, 2024

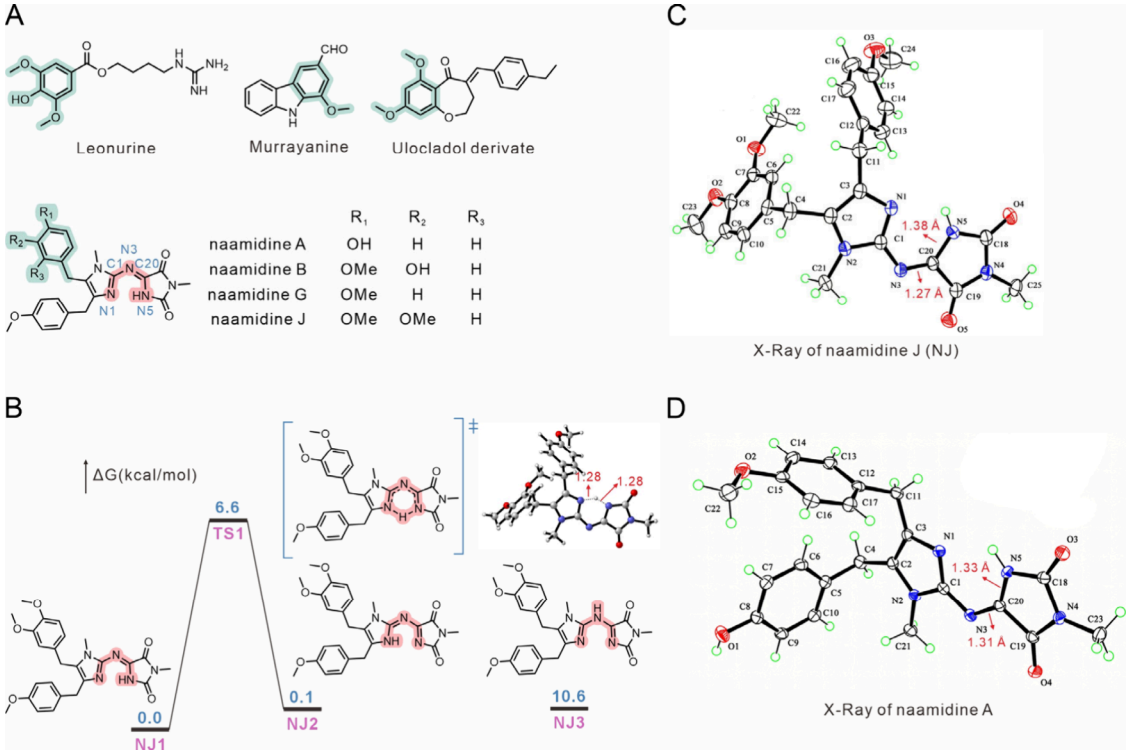

Figure 1. Structure confirmation and revision of marine natural products naamidines. (A) Chemical structures of leonurine, murrayanine, ulocladol derivate, naamidine A, B, G and J. (B) Calculation of NJ1 to NJ2 structural transition pathways and NJ3 energy at ωB97X-D/def2-TZVPP/PCM (acetonitrile)//B3LYP-D3(BJ)/6-31G(d)/PCM (acetonitrile). The bond distance is shown in Å. Free energy was shown in kcal/mol. (C, D) X-ray of naamidine J and naamidine A.

of proteins exert their unique bioactivity through nuclear translocation, especially transcription factor and histone deacetylase.[11,14] Meanwhile, post-translational modifications of many proteins are also required to enter the nucleus, such as phosphorylation of STAT3.[15] These biological events play unique roles in inflammation, proliferation, tumors, and metabolism. Previous studies have reported that CSE1L plays an important role in cell proliferation, apoptosis and epigenetic silencing.[10,11] However, there are few studies on the CSE1L role in inflammation. Furthermore, there are still no small molecules to regulate the function of CSE1L via interacting with CSE1L until now. Given the protein export function of CSE1L, it may be a promising target or strategy to regulate inflammation by targeting CSE1L.

In recent years, marine natural products (MNPs) have drawn great attention as valuable resources for drug discovery and novel target identification due to their unique structures and widespread biological activities associated with their special living circumstance.[16] Among them, marine alkaloids are the most promising lead compounds, since over half of the FDA-approved marine drugs are nitrogenous, such as Eribulin and Trabectedin.[17,18] Our group has long been dedicated to the discovery of bioactive MNPs and their related synthetic and pharmacological study, and during our research, naamidines attracted our attention due to their intriguing chemical scaffolds and widespread biological activities, such as anti-inflammatory, antiviral and cytotoxic effects.[19,20] Literature searching revealed that many methoxyphenyl-containing natural products or their derivatives have potential anti-inflammatory activities, such as leonurine, murrayanine and ulocladol derivatives.[21−23] Therefore, as they comprise two pieces of methoxyphenyl groups, an imidazole heterocycle and a hydantoin moiety, naamidines were worth being evaluated for their anti-inflammatory activities and explored for their possible novel functional target. In fact, naamidine J (NJ) has been previously isolated and synthesized by our group, and after comparing with the other naamidines, we found that the conjugation pattern between the imidazole ring and the hydantoin cycle was not uniform in different literature reports.[24−26] It is known to us that even tiny differences in the structure could have great influence on the bioactivities; thus, it is worth determining the conjugation patterns of these natural products, not only to solve the chemistry problem but also to be important for future drug design.

Herein, we reported the structure confirmation of NJ and related naamidine natural products by DFT calculation and X-ray diffraction analysis based on their isolation and rapid total synthesis. NJ was then found to inhibit LPS-induced inflammation in macrophages and acute lung injury for the first time. Leveraging photoaffinity labeling and proteomic techniques, CSE1L was identified as the direct functional target of NJ via activity-based protein profiling (ABPP). Mechanistic studies revealed that NJ directly bound to histidine (H) 745 and phenylalanine (F) 903 of CSE1L and inhibited the nuclear translocation and transcriptional activity of SP1 via CSE1L, followed by inhibiting the inflammatory response in macrophages and acute lung injury in mice. Taken together, in this study, we found CSE1L as a novel therapeutic target for macrophage-mediated inflammation and acute lung injury and highlighted a previously unknown role of CSE1L responsible for regulating the nuclear translocation and transcriptional activity of transcriptional factor SP1. Furthermore, we also provide a novel lead compound NJ for directly targeting CSE1L to ameliorate macrophage-mediated inflam-

https://doi.org/10.1021/jacs.4c09695
J. Am. Chem. Soc. 2024, 146, 28384−28397

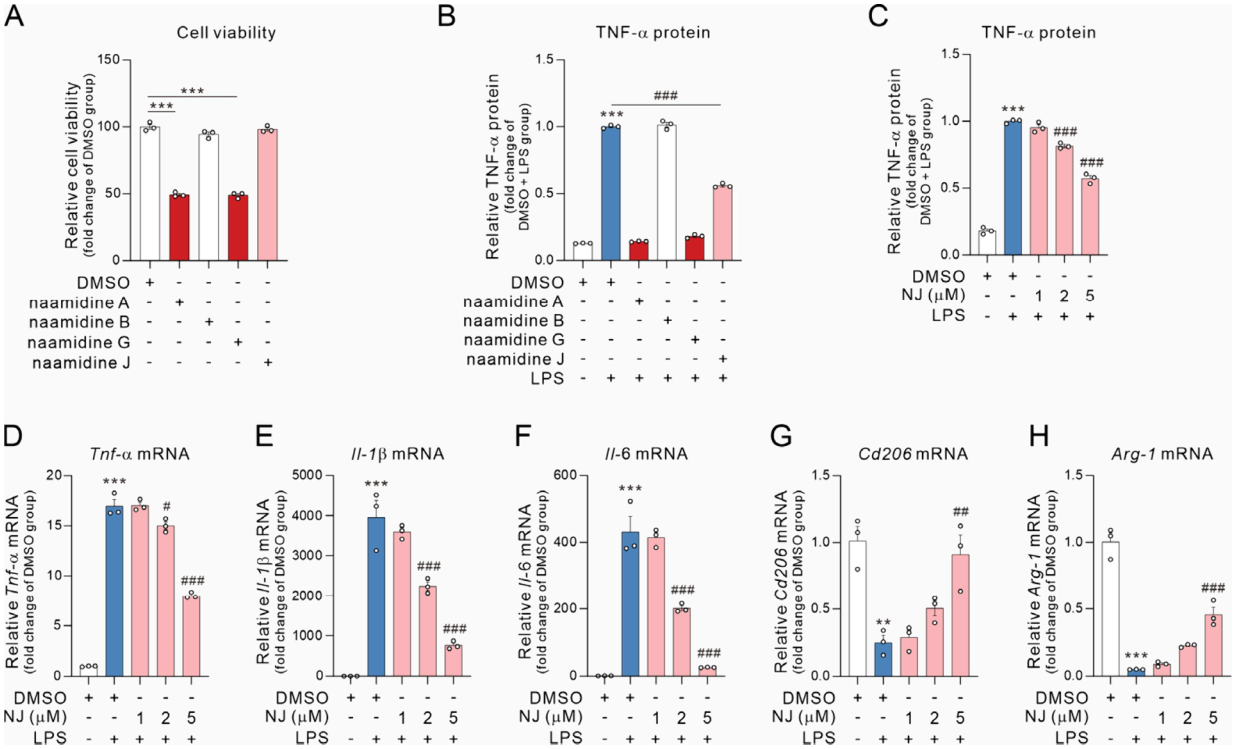

Figure 2. NJ inhibited the inflammatory response in LPS-induced macrophages. (A) Cell viability analysis of RAW264.7 macrophages treated with 5 μM of NJ and its analogs for 24 h, respectively. (B) ELISA analysis of TNF-α secretion in supernatants of LPS (100 ng/mL)-activated RAW264.7 macrophages treated with 5 μM of NJ and its analogs, respectively. (C) ELISA analysis of TNF-α secretion in supernatants of LPS-activated RAW264.7 macrophages treated with NJ at different concentrations. (D-F) qRT-PCR analysis of *Tnf-α*, *Il-1β* and *Il-6* mRNA expression of LPS (100 ng/mL)-induced macrophage treated with or without NJ. (G, H) qRT-PCR analysis of *Cd206* and *Arg-1* mRNA expression of LPS (100 ng/mL)-induced macrophage treated with or without NJ. Similar results were obtained from three independent experiments. All data are represented as mean ± SEM. Statistical analysis was carried out using One-way ANOVA followed by Tukey's posthoc test. $^{**}p < 0.01$ and $^{***}p < 0.001$ versus DMSO group; $^{\#}p < 0.05$, $^{\#\#}p < 0.01$ and $^{\#\#\#}p < 0.001$ versus DMSO + LPS group.

mation and acute lung injury. All of these indicated the potential research and development value of CSE1L, which may provide a novel target or drug candidate for the treatment of inflammatory disease, especially acute lung injury.

RESULTS

Discovery of NJ as a Potent Anti-inflammatory Agent in Macrophages and the Structure Confirmation and Revision of NJ and Its Related MNPs. To identify the promising anti-inflammatory leads, an in-house library of marine natural products and derivatives was screened for TNF-α inhibitory effects on RAW264.7 macrophages. About 50% of these compounds processed moderate anti-inflammatory bioactivity, with NJ showing the most potent anti-inflammatory bioactivity in our library (Figure S1, Supporting Information). NJ was previously isolated from marine sponges *Pericharax heteroraphis*,[20] and the total synthesis of NJ has been accomplished in our previous study.[27] However, when reviewing the structures of naamidines in the literature, e.g., naamidines A, B, G and J (Figure 1A), there are three conjugation patterns between the imidazole and the hydantoin, which should represent three different structures as shown in Figure 1B for NJ (NJ1−NJ3). Several studies have suggested that in this skeleton, the two double bonds were located between the N1 and C1 site, and the N5 and C20 site,[24] while other studies indicated that they were located between the N1 and C1 site, and the N3 and C20 site.[25] A few studies showed their location between the C1 and N3 site, and the N5 and C20 site (Figure S2A-C, Supporting Information).[26] However, there is no support for their correct double bond positions with convincing data, such as single crystal structure data. Since the structure variations of small molecules have always had a great influence on their bioactivities, and for the sake of future possible structure-based drug design and target fishing, we decided to further confirm the structures of naamidines. In this study, three potential structures of NJ were evaluated through density functional theory (DFT) calculations. The results indicated relative Gibbs free energies of 0.0, 0.1, and 10.6 kcal/mol for NJ1, NJ2, and NJ3, respectively, with NJ3 displaying significantly higher energy (Figure 1B; Supplementary Table 1). This thermodynamic instability suggests that the structure of NJ3 is incorrect. To determine the most stable configuration of NJ, the single crystal was grown and analyzed and crystallographic examination revealed a shorter N3−C20 bond length compared to N5−C20 (1.27 Å < 1.38 Å), confirming NJ1 was the thermodynamically preferred structure (Figure 1C). Furthermore, according to previous methods,[27,28] naamidines A, B and G were synthesized, and fortunately we also obtained the single crystal of naamidine A, which confirmed the double bonds of these naamidine molecules should all be N3−C20 (Figure 1D). Besides, the DFT calculations also supported the above results (Figure S2D, Supporting Information; Supplementary Table 1). It is worth noting that the structure patterns NJ1 and NJ2 could possibly tautomerize to each other in the solvent, but the form NJ3 should not exist based on the above evidence, and such

https://doi.org/10.1021/jacs.4c09695
J. Am. Chem. Soc. 2024, 146, 28384−28397

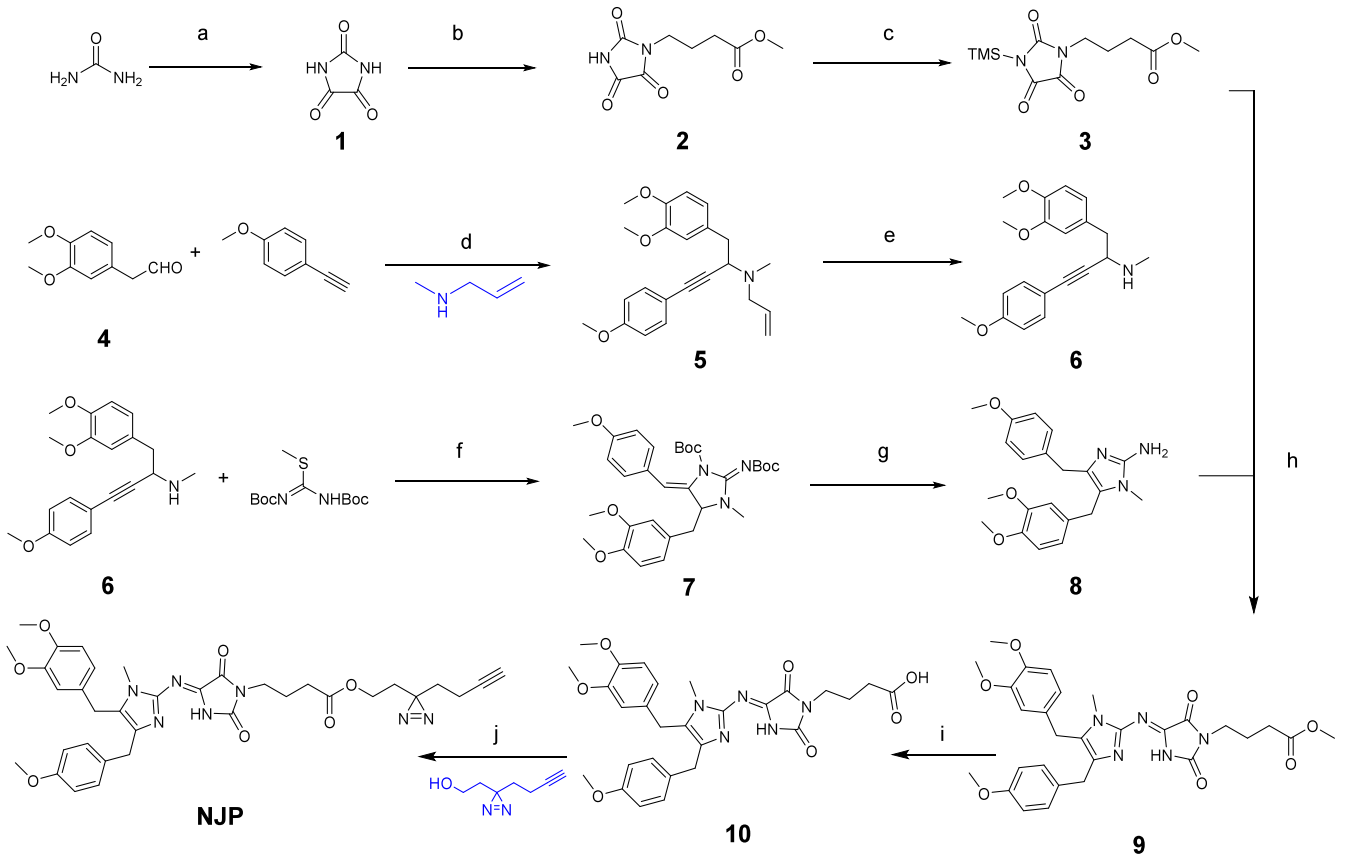

Figure 3. Synthesis of photoaffinity probe NJP. Reagents and reaction conditions: (a) Oxalyl chloride, THF, rt, 5 h, 98%; (b) Methyl 4-bromobutyrate, NaH, DMF, 12 h, 76%; (c) *N,O*-Bis(trimethylsilyl)acetamide, CH_3CN, reflux, 5 h; (d) (1), Toluene, 4 Å MS, reflux, 120 °C, 12 h, (2), CuBr, 36 h, 86%; (e) $Pd(PPh_3)_4$, 1,3-DMBA, DCM, rt, 12 h, 79%; (f) $AgNO_3$, Et_3N, MeCN, rt, 5−20 min, 91%; (g) TFA/H_2O (v/v = 1:2), rt, 3 h, 81%; (h) Toluene, reflux, 14 h, 65%; (i) LiOH, THF/H_2O (v/v = 3:1), rt, 94%; (j) EDC, DCM, rt, 86%.

drawing of NJ-related compounds should be wrong. Our results showed that the double bonds of these naamidine molecules should be N3−C20, which confirmed those reports with the right drawings and revised those with the wrong ones. These findings have provided useful guidelines for the subsequent structural characterization of this series of compounds and their future possible structure−activity relationship (SAR) analysis.

NJ Inhibited the Inflammatory Response in LPS-induced Macrophages. In the early phase of acute lung injury, immune cells, such as macrophages, produce large amounts of inflammatory cytokines which in turn damage lung tissues.[3,5] Reducing the inflammatory response of macrophages is an effective strategy to ameliorate early acute inflammatory disease, such as acute lung injury.[6] Inspired by the anti-inflammatory bioactivity of NJ analogs and their intriguing structures,[19] we further conducted an anti-inflammatory bioactivity phenotypic screening of NJ analogs in LPS-induced RAW264.7 macrophages together with other MNPs and derivatives in our compound library. NJ showed significant anti-inflammatory activity in RAW264.7 macrophages and is not toxic to macrophages compared to other analogs (Figure 2A, B). After determining the precise structure of NJ, we evaluated its anti-inflammatory bioactivity at the *in vitro* cellular level. In RAW264.7 macrophages, we observed that NJ dose-dependently reduced LPS-induced TNF-α cytokine secretion into the culture medium of RAW264.7 macrophages (Figure 2C). CCK-8 assay showed that NJ did not affect cell viability under either physiological or pathological conditions of macrophages (Figure S3A, B, Supporting Information). In addition, NJ also dose-dependently inhibited LPS-induced upregulation of pro-inflammatory cytokines, such as *Tnf-α*, *Il-1β* and *Il-6* mRNA (Figure 2D-F). Conversely, NJ also significantly reversed the LPS-induced downregulation of anti-inflammatory cytokines such as *Cd206* and *Arg-1* mRNA (Figure 2G, H). Furthermore, in LPS-induced THP-1 cells, NJ also demonstrated a similar anti-inflammatory effect as in RAW264.7 macrophages (Figure S4A-G, Supporting Information). Taken together, these results indicate that NJ shows a promising biological activity against inflammation in macrophages.

Identification of CSE1L as a Direct Target of NJ in Macrophage. To further clarify the mechanism of the anti-inflammatory bioactivity of NJ, we synthesized a molecular probe (NJP) based on NJ by introducing a difunctional side chain with a diazirine and an alkyne (Figure 3). The alkyne was conjugated with the reporter biotin-PEG_3-N_3 or TAMRA-PEG_3-N_3 via a Cu (I)-catalyzed azide−alkyne click chemistry reaction.[29,30] Meanwhile, the diazirine chemical group was used to covalently bind the target proteins of macrophage via photoaffinity labeling.[31] The chemical structure of NJP was verified by ^1H NMR, ^{13}C NMR spectra and high-resolution mass spectrometry, which suggested that the difunctional side chain was linked on the NJ skeleton (Figure 3).

We first tested whether the diazirine chemical group affects the anti-inflammatory bioactivity of NJ and whether NJP can

https://doi.org/10.1021/jacs.4c09695
J. Am. Chem. Soc. 2024, 146, 28384−28397

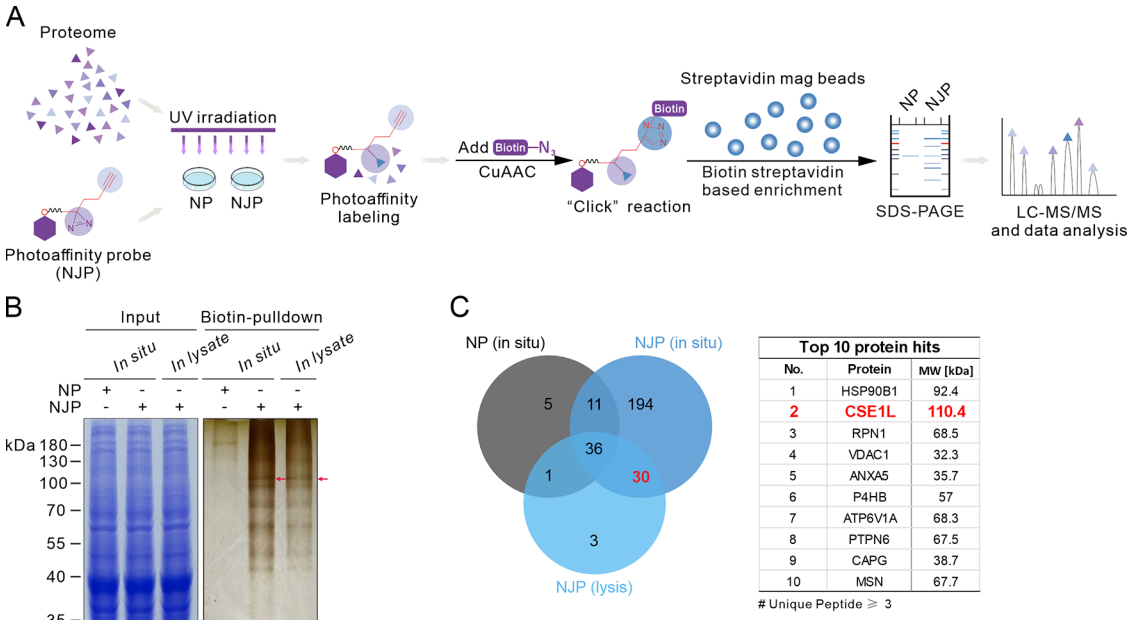

Figure 4. Target identification of NJ in macrophages by activity-based protein profiling (ABPP). (A) Schematic illustration of target protein capture of NJ in macrophages based on ABPP. (B) Silver staining shows NJP-captured proteins in macrophages, and Coomassie brilliant blue staining was used to be an input control. (C) Venn diagram showing the possible target proteins that were significantly enriched by photoaffinity probe NJP in macrophages, and the top 10 hits were shown in the right table.

be used for target identification of NJ. To compare the bioactivity between NJ and NJP, CCK-8 and ELISA assays were performed by NJ or NJP treatment, respectively, followed by LPS stimulation in RAW264.7 macrophages. The results indicate that NJP shows similar anti-inflammatory bioactivity compared with NJ in RAW264.7 macrophages and is suitable for target identification of NJ in macrophages (Figure S5A and B, Supporting Information).

Next, the target identification of NJ in macrophages based on activity-based protein profiling (ABPP) was performed. The workflowchart of protein target identifications is shown in Figure 4A and based on a previous report.[23] RAW264.7 macrophages were treated with NP or NJP, respectively, and then exposed to UV irradiation. After UV irradiation, the cell lysates were prepared and followed by being clicked with Biotin-PEG_3-N_3 via click reaction. Then, the NJP-captured proteins were pulled down by streptavidin beads, followed by silver staining (Figure 4B), and then the whole bands were subjected to digestion with sequencing grade modified trypsin (Promega) followed by liquid chromatography tandem-mass spectrometry (LC-MS/MS) analysis. The amounts of proteins were identified, and CSE1L, an obvious band in Figure 4B, which is also named XPO2 or exportin-2, drew our attention (Figure 4C). Besides, the further pull-down experiments suggested that CSE1L was pulled down by NJP and significantly blocked with an excess amount of NJ for competition (Figure 5A), and CRM1, which is also named XPO1 or exportin-1, could not be pulled down by NJP via the click reaction and streptavidin beads in macrophages (Figure 5A). In addition, the cellular thermal shift assay showed that NJ could enhance the thermal stability of CSE1L in macrophages (Figure 5B). Furthermore, the surface plasmon resonance (SPR) assay indicated that NJ directly bound to CSE1L, and the K_D value is 5.41 μM (Figure 5C). These results suggested that NJ could bind with CSE1L at both the protein level and cellular level.

Furthermore, to verify the role of CSE1L in inflammation in macrophages, the pLKO.1-shCSE1L-copGFP-Puro plasmid was designed and constructed. The knockdown efficiency of the plasmid was confirmed through immunoblotting as shown in Figure 5D-F. The ELISA assay suggested that knockdown of CSE1L in macrophages could decrease the release of TNF-α cytokine (Figure 5G), which means that CSE1L deficiency inhibits inflammation in macrophages. Besides, it is interesting to note that NJ treatment fails to further decrease TNF-α cytokine release in CSE1L knockdown macrophages compared to knockdown CSE1L in macrophages (Figure 5G), suggesting that NJ inhibits inflammation in macrophages via the CSE1L protein target. All these results reveal that CSE1L protein is a direct target of NJ on its anti-inflammatory bioactivity in macrophages.

The H745 and F903 Are the Key Residues Responsible for the Binding Between NJ and CSE1L. Based on the principle of chemical probes, NJP and NJ showed similar anti-inflammatory activities in macrophages (Figure S5B, Supporting Information), and excess NJ decreased the pull-down of CSE1L by NJP for competition (Figure 5A), which suggests that NJP and NJ located the same binding pockets of CSE1L. To determine the specific NJ binding sites on CSE1L protein, the NJ molecular probe (NJP) was incubated with purified CSE1L protein for 30 min at room temperature, followed by UV irradiation on ice. Then, NJP was covalently cross-linked with CSE1L at the binding sites by photoaffinity diazirine (Figure 6A, B). The NJP-CSE1L complex was digested with sequencing grade modified trypsin (Promega) and then subjected to LC-MS/MS analysis. A 110.07316 Da

https://doi.org/10.1021/jacs.4c09695
J. Am. Chem. Soc. 2024, 146, 28384−28397

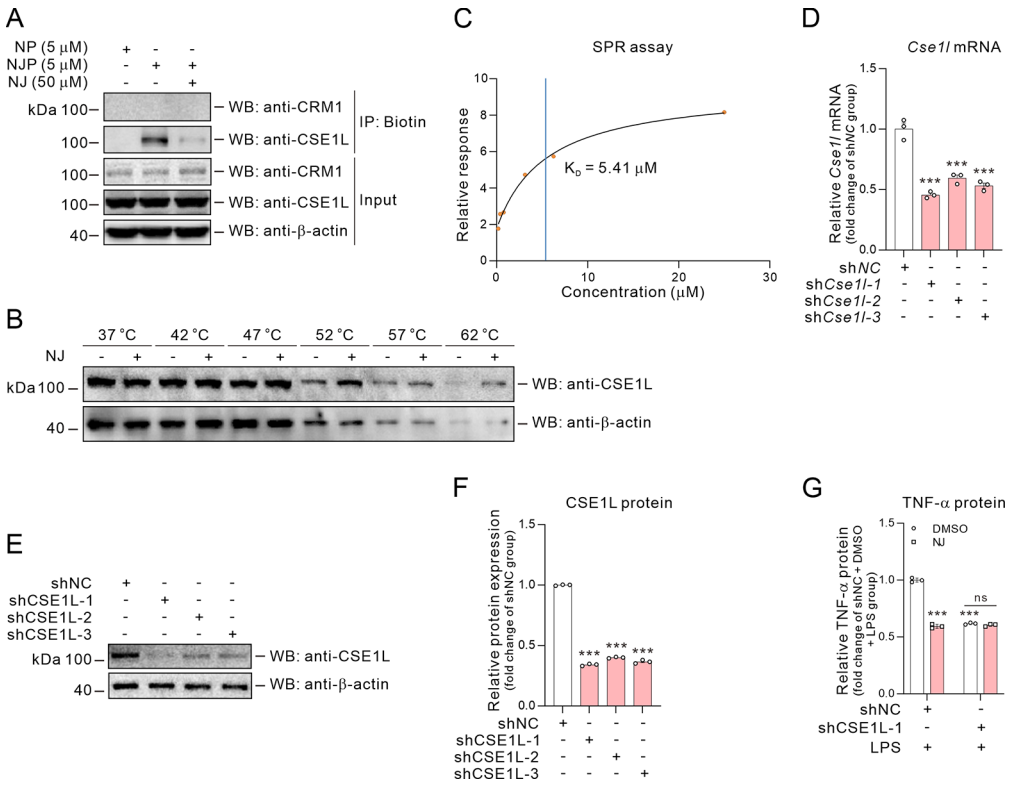

Figure 5. CSE1L serves as a target protein of NJ. (A) Pull-down analysis of NJ-binding to CSE1L in macrophages. (B) CETSA analysis of intracellular binding between NJ (5 μM) and CSE1L. (C) Surface plasmon resonance (SPR) analysis of interactions between NJ and CSE1L, and the K_D value was 5.41 μM. (D-F) qRT-PCR and immunoblotting analysis of CSE1L expression in macrophages by shCSE1L lentivirus transfection. (G) Knockdown of CSE1L reversed the NJ (5 μM) anti-inflammatory activity in macrophages. Similar results were obtained from three independent experiments. All data are represented as mean ± SEM. Statistical analysis was carried out using One-way ANOVA followed by Tukey's posthoc test (D, F). Statistical analysis was carried out using Two-way ANOVA followed by Bonferroni's posthoc test (G). Three-asterisk indicates $p < 0.001$.

($C_7H_{10}O^-$) increase in molecular weight of the peptide of CSE1L proteins, corresponding to the photoactivated cleaved fragment, was detected to bind at serine (S) 762 and valine (V) 763 of the peptide 742-ANDHQGFYLLNSIIEHMPPE-SVDQYR-767 (Figure 6C), suggesting that the possible binding sites of NJ may fall into the pocket where this peptide is located. To map the binding reactions between NJ and CSE1L, we docked NJ into the structure of CSE1L, created by AlphaFold2, around the residues 742−767 aa. The preferential binding modes were generated (Figure 6D-F), and the algorithm predicts that NJ binds to the pocket of CSE1L. Two hydrogen bonds (histidine (H) 745 and phenylalanine (F) 903) and one Pi-Pi stacking (glutamate (E) 888) may play a key role in the interaction between NJ and CSE1L (Figure 6E, F). All of these residues were in the pocket where the N-terminal 742−767 aa regions are located. Interestingly, mutating H745 and F903 to alanine (A), respectively, almost completely destroyed the binding between NJ and CSE1L but mutating E888 to alanine (A) did not affect the interaction between NJ and CSE1L (Figure 6G). Meanwhile, the DARTS assay also showed that NJ restrained the proteolysis of CSE1L (WT) and CSE1L (E888A) by Pronase but could not restrain the proteolysis of CSE1L (H745A) and CSE1L (F903A) by Pronase (Figure 6H). Therefore, these results further prove that two key residues histidine (H) 745 and phenylalanine (F) 903 are responsible for the interaction of NJ and CSE1L.

NJ Inhibits Nuclear Translocation of Transcription Factor SP1 Mediated by CSE1L. Given that the functional role of NJ and CSE1L in inflammation is poorly understood, we further explored how NJ inhibits inflammation in macrophages via targeting CSE1L. CSE1L is the human homologue of the yeast chromosome segregation gene, CSE1, and it encodes a 971-amino acid protein with approximate 100 kDa molecular masses distributing in the cytoplasm and nuclei of cells.[32] As its yeast counterpart, CSE1, the human CSE1L protein also functions as a nuclear transport (export) factor. Previous studies reported that CAS mediates the nuclear to cytoplasmic recycling of importin α.[10] CSE1L and importin α coregulate nuclear and cytoplasmic translocation of proteins and RNA, such as transcription factor, histone and circular RNA.[10−12] We first detected the effect of NJ on the protein expression of CSE1L, and the results showed that NJ shows no effect on the protein expression of CSE1L regardless of the physiological or pathological conditions (Figure S6A and B, Supporting Information). Besides, we found that NJ was predominantly distributed in the cytoplasm in LPS-induced macrophages, and NJ treatment slightly decreased CSE1L expression in the nucleus (Figure S6C, Supporting Information). Since CSE1L functions as a nuclear transport factor, we are interested in its possible cargo proteins that may translocate between the nucleus and cytoplasm in macrophages after NJ treatment under LPS stimulation. Thus, an unbiased quantitative proteomics approach was used to dissect the pathway or CSE1L cargoes affected by NJ (Figure 7A). After quantification of the partitioning of proteins between the cytoplasm and nucleus in macrophages after NJ and LPS

https://doi.org/10.1021/jacs.4c09695
J. Am. Chem. Soc. 2024, 146, 28384−28397

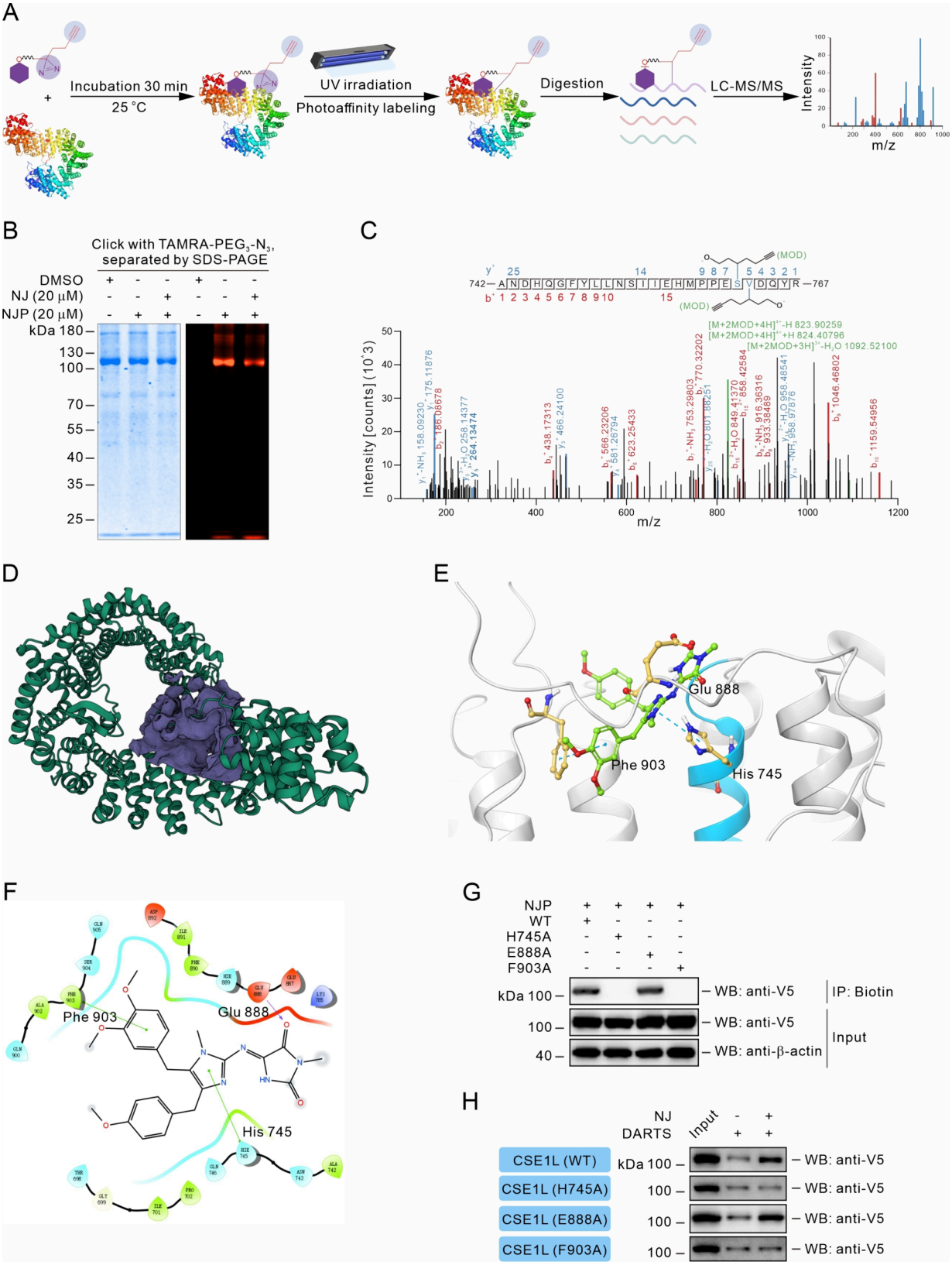

Figure 6. Mapping the binding sites of NJ on CSE1L. (A) Overall schematic illustration of binding site identification between NJ and CSE1L. (B) In-gel fluorescence scanning shows NJP could bind with CSE1L protein, and this binding could be inhibited by the parent compound NJ. (C) LC-MS/MS analysis of the photoaffinity labeling peptides by NJP on CSE1L. (D) The binding pocket where the NJP-binding peptide of CSE1L is located. (E, F) Docking model of NJ into the structure of CSE1L. (G) The pull-down experiments between NJP (5 μM) and CSE1L (WT), CSE1L (H745A), CSE1L (E888A) or CSE1L (F903A) in HEK293T cells. (H) Immunoblotting analysis of the binding between NJ (5 μM) and CSE1L (WT), CSE1L (H745A), CSE1L (E888A) or CSE1L (F903A) via DARTS in HEK293T cells. Pronase: Protein (w/w) = 1:250. Similar results were obtained from three independent experiments.

https://doi.org/10.1021/jacs.4c09695
J. Am. Chem. Soc. 2024, 146, 28384−28397

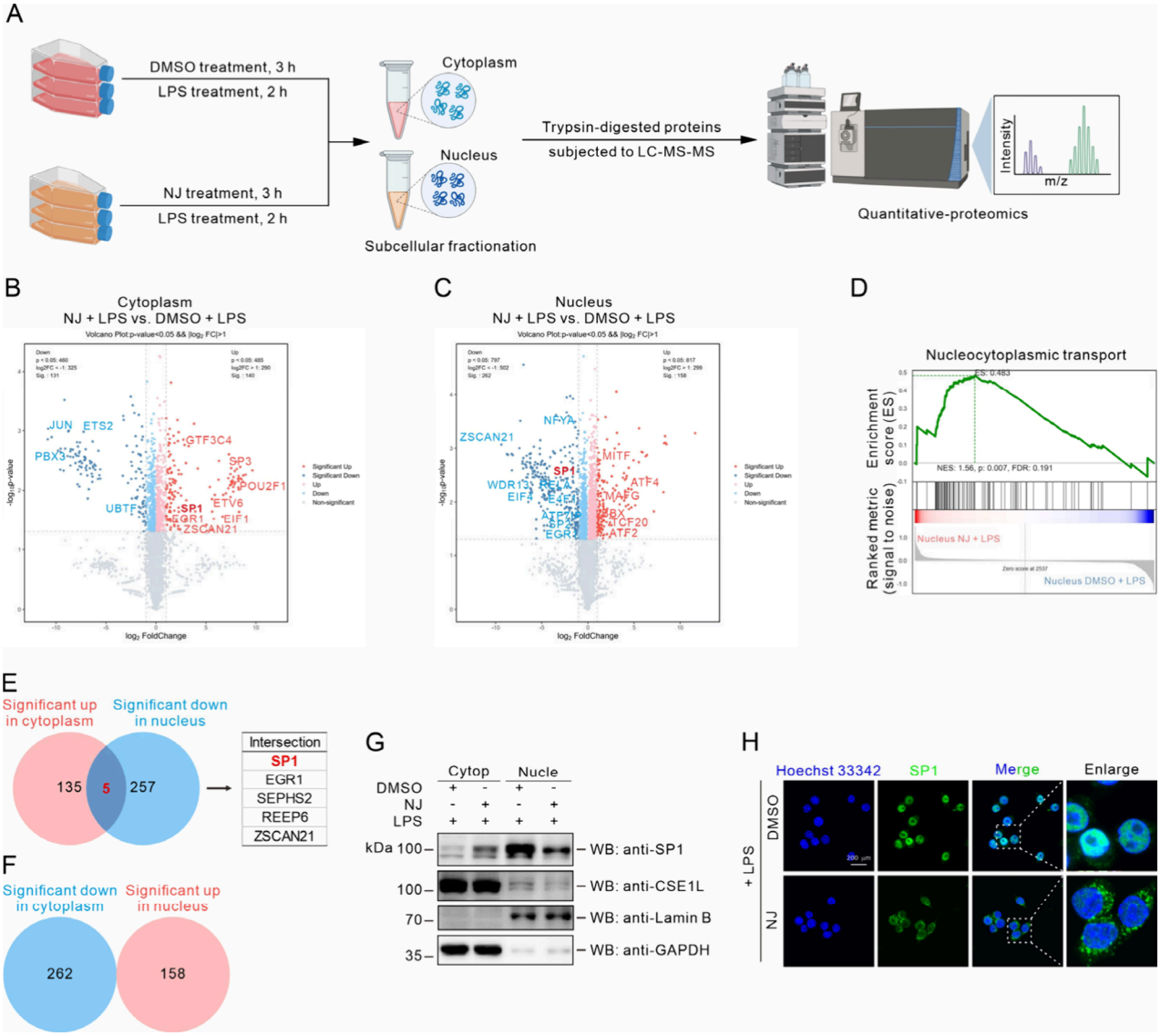

Figure 7. NJ promotes transcriptional factor SP1 cytoplasmic accumulation in LPS-induced macrophages. (A) Schema of quantitative proteomics analysis of cytoplasmic and nuclear proteins in LPS (100 ng/mL)-activated macrophages treatment with vehicle (DMSO) or NJ (5 μM). (B, C) Volcano plots of differential protein abundance in the cytoplasm and nucleus of LPS-activated macrophages treated with NJ (5 μM) versus vehicle (DMSO). (D) Gene-set enrichment analysis (GSEA) of the nucleocytoplasmic transport target protein signatures in LPS-induced macrophages treated with NJ (5 μM), as compared to the vehicle (DMSO). (E) Venn diagram showing the proteins with significant upregulation in cytoplasm and with significant downregulation in nucleus, and the intersection were shown in the right table. (F) The diagram showing no protein with simultaneously significant downregulation in the cytoplasm and significant upregulation in the nucleus. (G) Immunoblotting analysis of target protein CSE1L and transcriptional factor SP1 in cytoplasm and nucleus of LPS-induced macrophages treated with NJ (5 μM) or vehicle (DMSO). (H) Immunofluorescence analysis of transcriptional factor SP1 in cytoplasm and nucleus of LPS-induced macrophages treated with NJ (5 μM) or vehicle (DMSO). Scale bars = 200 μm. Similar results were obtained from three independent experiments (G, H).

treatment, we identified several proteins as significantly differentially distributed after NJ and LPS treatment (p-value < 0.05 and |$\log_2$ FC| > 1, Figure 7B, C), and which include numerous members of transcription factor, such as SP1, EGR1, JUN, PBX3, ETS2, et al. (Figure 7B, C). In addition, the GSEA analysis suggested that the nucleocytoplasmic transport pathway, which includes CSE1L, the target proteins of NJ significantly changed after NJ and LPS treatment (Figure 7D). Furthermore, the GO analysis indicated that the biological events regulated by NJ mainly focused on transcriptional regulation (Figure S7A and B, Supporting Information). Therefore, we mainly analyzed the proteins, especially transcription factors, which were altered between the nucleus and cytoplasm of macrophages subjected to NJ treatment and LPS stimulation. The proteomic analysis results showed that several proteins shuttle between the nucleus and cytoplasm. SP1, EGR1, SEPHS2, REEP6, ZSCAN21 were significantly upregulated in the cytoplasm and downregulated in the nucleus at the same time (Figure 7E), but no protein was downregulated in the cytoplasm and upregulated in the nucleus at the same time after NJ treatment (Figure 7F). Our immunoblotting analysis also indicated that NJ treatment resulted in the accumulation of SP1 in the cytoplasm in the LPS-induced macrophages (Figure 7G). Besides, the results of the immunofluorescence images were also consistent with these findings (Figure 7H). All of these results suggested that

https://doi.org/10.1021/jacs.4c09695
J. Am. Chem. Soc. 2024, 146, 28384−28397

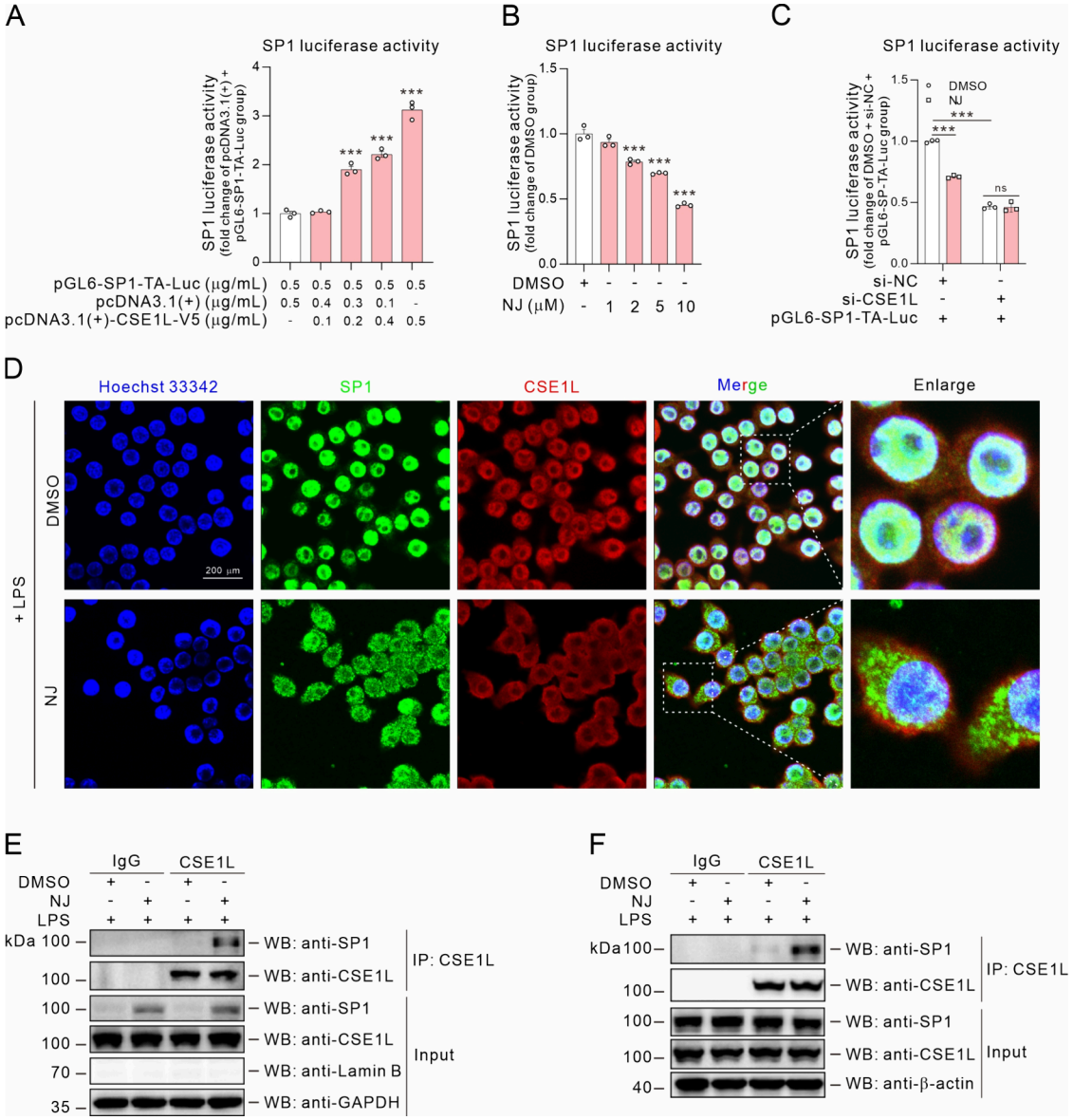

Figure 8. NJ inhibits the transcriptional activity of SP1 via CSE1L. (A) Overexpression of CSE1L promoted the transcriptional activity of SP1. (B) NJ inhibited the transcriptional activity of SP1. (C) Knockdown of CSE1L reversed the NJ (5 μM)-inhibited SP1 transcriptional activity. (D) Immunofluorescence assay of the colocation of CSE1L and SP1 in LPS-induced macrophages treated with NJ (5 μM) or vehicle (DMSO). Scale bars = 200 μm. (E) Immunoprecipitation assay of the interaction in cytoplasm fraction between CSE1L and SP1 in LPS-induced macrophages treated with NJ (5 μM) or vehicle (DMSO). (F) Immunoprecipitation assay of the interaction in whole cell lysate between CSE1L and SP1 in LPS-induced macrophages treated with NJ (5 μM) or vehicle (DMSO). Similar results were obtained from three independent experiments. All data are represented as mean ± SEM. Statistical analysis was carried out using One-way ANOVA followed by Tukey's posthoc test (A, B). Statistical analysis was carried out using Two-way ANOVA followed by Bonferroni's posthoc test (C). Three-asterisk indicates $p < 0.001$.

NJ treatment inhibits nuclear translocation of transcriptional factor SP1 in macrophages followed by LPS treatment.

NJ Inhibits the Transcriptional Activity of SP1 via CSE1L. SP1 is a eukaryotic specific factor, which was also considered a general transcription factor, and the full-length SP1 protein is highly conserved among mammalian species,[33,34] and previous studies have shown that SP1 plays an important role in metabolism, cell proliferation/growth, cell death, and inflammation.[33,35−37] Previous studies have shown that inhibition of SP1 could attenuate airway inflammation via suppressing the SP1/FGFR3/PI3K/AKT axis,[35] or inhibit acute inflammation by the SP1/TLR2/NF-κB axis,[38] or inhibit adjuvant-induced arthritis via the HDAC6/MyD88/NF-κB pathway,[37] which suggested that inhibition of SP1 could mitigate an inflammatory response via multiple signaling pathways. Therefore, we constructed a luciferase reporter gene assay to detect the SP1 transcriptional activity. The results suggested that CSE1L could promote the transcriptional activity of SP1 (Figure 8A; Figure S8A, Supporting Information), while NJ could inhibit the transcriptional activity of SP1 (Figure 8B). Since CSE1L functions as a direct target protein of NJ, we wondered whether there is a regulation role of NJ on SP1 transcriptional activity via CSE1L. Therefore, we further detected the inhibitory effect of NJ on SP1 transcriptional activity in CSE1L knockdown cells. We found that knockdown of CSE1L reversed the NJ-inhibited SP1 transcriptional activity (Figure 8C; Figure S8B, Supporting Information). These results showed that NJ inhibited SP1

https://doi.org/10.1021/jacs.4c09695
J. Am. Chem. Soc. 2024, 146, 28384−28397

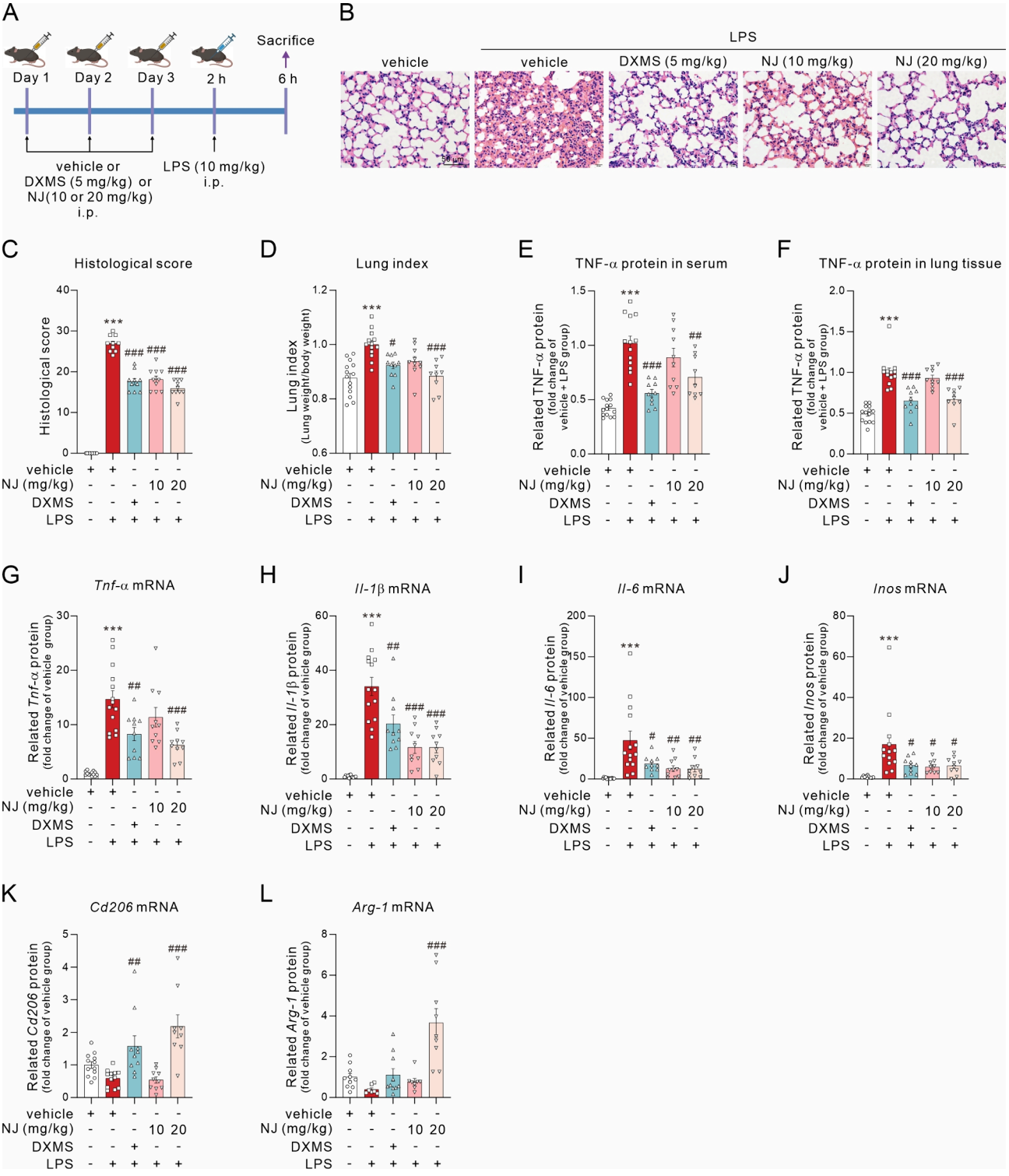

Figure 9. NJ alleviates LPS-induced lung injury in mice. (A) Experimental design to study the effects of NJ against LPS-induced lung injury in mice. (B, C) H&E staining and histological score of lung tissues from LPS-induced mice administrated with NJ or vehicle (5% DMSO + 15% Kolliphor HS 15 + 80% Normal saline) (n = 10). (D) Lung index of LPS-induced mice administrated with NJ or vehicle (n = 9−14). (E, F) ELISA analysis of TNF-α protein in serum and lung tissues from LPS-induced mice with lung injury administrated with NJ or vehicle (n = 9−14). (G−J) qRT-PCR analysis of pro-inflammatory cytokines (*Tnf-α, Il-1β, Il-6* and *Inos*) expression of lung tissue of mice with lung injury administrated with NJ or vehicle (n = 9−14). (K−L) qRT-PCR analysis of anti-inflammatory cytokines (*Cd206* and *Arg-1*) expression of lung tissue of mice with lung injury administrated with NJ or vehicle (n = 8−12). All data are represented as mean ± SEM. Statistical analysis was carried out using One-way ANOVA followed by Tukey's posthoc test. $^{***}p < 0.001$ versus vehicle group; $^{\#}p < 0.05$, $^{\#\#}p < 0.01$ and $^{\#\#\#}p < 0.001$ versus vehicle + LPS group.

transcriptional activity via CSE1L. Besides, immunofluorescence experiments suggested that NJ could increase the colocation of CSE1L and SP1 in the cytoplasm of LPS-activated macrophages (Figure 8D). Besides, the immunoprecipitation experiments further showed that CSE1L could directly interact with SP1, and NJ could promote the

https://doi.org/10.1021/jacs.4c09695
J. Am. Chem. Soc. 2024, 146, 28384−28397

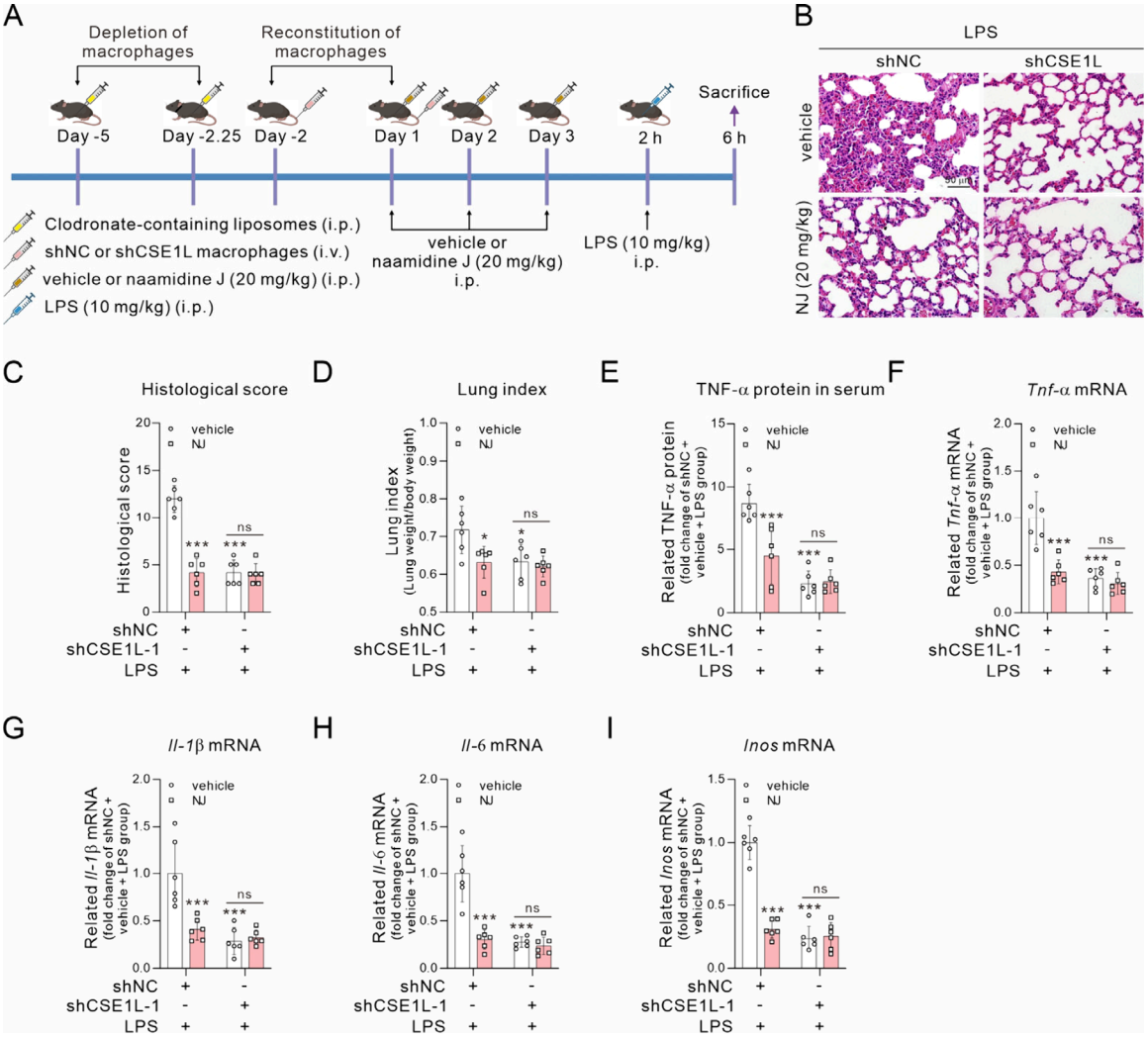

Figure 10. CSE1L was a necessary target responsible for the improvement of the acute lung injury of NJ. (A) Experimental design to study whether the therapeutic effect of NJ is dependent on CSE1L in LPS-induced acute lung injury *in vivo*. (B, C) H&E staining and histological score of lung tissues from LPS-induced mice reconstituted of CSE1L-knockdown macrophages in the presence or absence of NJ treatment (n = 6). (D) Lung index of LPS-induced mice reconstituted of CSE1L-knockdown macrophages in the presence or absence of NJ treatment (n = 6). (E) ELISA analysis of TNF-α protein in serum from LPS-induced mice reconstituted of CSE1L-knockdown macrophages in the presence or absence of NJ treatment (n = 6). (F−I) qRT-PCR analysis of pro-inflammatory cytokines (*Tnf-α*, *Il-1β*, *Il-6* and *Inos*) expression of lung tissue of LPS-induced mice reconstituted of CSE1L-knockdown macrophages in the presence or absence of NJ treatment (n = 6). All data are represented as mean ± SEM. Statistical analysis was carried out using Two-way ANOVA followed by Bonferroni's posthoc test. One-asterisk indicates $p < 0.05$, two-asterisk indicates $p < 0.01$ and three-asterisk indicates $p < 0.001$.

interaction between CSE1L and SP1 in LPS-activated macrophages (Figure 8E, F). These results indicated that NJ binding to CSE1L could cooperatively promote the cytoplasmic accumulation of SP1, which in turn inhibits the transcriptional activity of SP1, followed by suppressing inflammation in macrophages.

NJ Protects Against LPS-induced Acute Lung Injury *in vivo* Depending on CSE1L. Reducing or intervening the inflammatory response in the lung is an early well-proven strategy for the treatment of acute lung injury and acute respiratory distress syndrome.[3−5] Besides, previous study had uncovered that SP1 reduced the nuclear localization of HNF4α and induced ACE2 expression, and further resulted in enhanced viral replication and tissue injury infected with SARS-CoV-2,[39] which revealed that SP1 may play an indispensable role in lung injury. Thus, we performed an *in vivo* animal experiment to assess the anti-inflammatory effects of NJ in an LPS-induced acute lung injury (Figure 9A). As shown in the Hematoxylin and eosin (H&E) staining assay, NJ significantly ameliorated the damage of lung tissue of mice subjected to LPS (Figure 9B, C). Meanwhile, NJ treatment also reduced pulmonary edema in mice (Figure 9D). ELISA assay suggested that NJ treatment decreased the expression of TNF-α cytokine in the lung tissue and serum of mice (Figure 9E, F). Further evaluation of inflammatory markers showed that NJ treatment significantly ameliorated lung injury of mice, which embodied the decrease of pro-inflammatory cytokines (*Tnf-α*, *Il-1β* and *Il-6* mRNA) (Figure 9G-J) and the increase of anti-inflammatory cytokines (*Cd206* and *Arg-1* mRNA) (Figure 9K, L). Besides, we also investigated the ratio of M1/M2 macrophages in the lung by flow cytometry. The results revealed that the percentage of $CD45^+CD11b^+F4/80^+CD86^+$ M1 macrophages was significantly increased and the percentage of $CD45^+CD11b^+F4/80^+CD206^+$ M2 macrophages

https://doi.org/10.1021/jacs.4c09695
J. Am. Chem. Soc. 2024, 146, 28384−28397

in the lung was slightly decreased after LPS injection (Figure S9A-C, Supporting Information). However, NJ administration (20 mg/kg) reduced M1 macrophages and increased M2 macrophages in the lungs of mice subjected to LPS (Figures S9A-C, Supporting Information). In addition, the depletion and reconstitution of CSE1L-knockdown macrophages experiments in mice were performed to reveal the role of CSE1L in acute lung injury (Figure 10A). Lung macrophages were depleted about 70% after injection with clodronate-containing liposomes compared to injection with control liposomes (Figure S10A and B, Supporting Information). Lentivirus-packaged shCSE1L-1 significantly inhibited CSE1L expression in BMDMs (Figure S10C, Supporting Information). Then, the macrophages adoptive transfer experiments were performed to demonstrate whether NJ protects against LPS-induced acute lung injury *in vivo* depending on CSE1L. Our results showed that CSE1L expression in macrophages isolated from lung of mice deprived of their own macrophages and reconstituted of CSE1L-knockdown macrophages was decreased compared to those of isolated from lung of mice deprived of their own macrophages and reconstituted of normal control macrophages (Figure S10D, Supporting Information), which suggested that CSE1L was knocked down in the macrophages of lung in mice. The macrophage adoptive transfer experiments mediated by lentivirus showed that the wide type mice deprived of their own macrophages and reconstituted of CSE1L-knockdown macrophages could protect against acute lung injury induced by LPS. The results indicated that CSE1L deficiency in macrophages could improve the symptoms of LPS-induced acute lung injury, including the reduced inflammatory cell infiltration in the lung, the lung/weight index, and the inflammatory cytokine expression (Figure 10B–I). Moreover, we found that mice deprived of their own macrophages and reconstituted of CSE1L-knockdown macrophages, followed by treatment with NJ, simultaneously did not exert significant improvement effect compared with the mice that were only deprived of their own macrophages and reconstitution of CSE1L-knockdown macrophages (Figure 10B–I). These results indicated that NJ ameliorated acute lung injury mainly via CSE1L *in vivo*. Altogether, these findings indicated a novel pharmacological role of a marine natural product NJ for the treatment of acute lung injury and also provided a lead compound or an available chemical tool for investigating CSE1L biological function and developing novel drug candidates against inflammatory disease, such as acute lung injury.

CONCLUSION

In this study, for the first time, we reported that NJ inhibited the LPS-induced inflammatory response in macrophages and ameliorated acute lung injury in mice, and we also identified CSE1L as the direct cellular target protein of NJ for anti-inflammatory bioactivity via ABPP. Besides, the structures of NJ and related naamidine type MNPs were confirmed or revised by DFT calculation and X-ray diffraction analysis, which was helpful for further chemical and biological study. Moreover, we found that the histidine (H) 745 and phenylalanine (F) 903 of CSE1L protein are essential for the binding between NJ and CSE1L. Given that CSE1L protein functions as a nuclear transport (export) factor in cells,[10] we conducted an unbiased proteomics to dissect the CSE1L cargoes after NJ treatment in LPS-activated macrophages. Eventually, we found that NJ inhibited SP1 nuclear translocation via CSE1L, further inhibited SP1 transcriptional activity and inflammation in macrophages, and ameliorated acute lung injury *in vivo*. Therefore, these findings provide a novel perspective for exploring CSE1L biology in inflammation and enable a new lead compound such as the marine natural product NJ for innovative drug discovery for inflammatory diseases including acute lung injury.

EXPERIMENTAL SECTION

Supporting Materials and Methods and Supporting Data are provided in the Supporting Information.

ASSOCIATED CONTENT

Data Availability Statement

The data that support the findings of this study are available from the corresponding author upon reasonable request.

Supporting Information

The Supporting Information is available free of charge at https://pubs.acs.org/doi/10.1021/jacs.4c09695.

Part I: Chemistry experimental section; Part II: Bioactivity experimental procedures; Part III: Supplementary tables and figures (PDF)

AUTHOR INFORMATION

Corresponding Authors

Xu-Wen Li − *State Key Laboratory of Chemical Biology, Drug Discovery and Design Center, Shanghai Institute of Materia Medica, Chinese Academy of Sciences, Shanghai 201203, P. R. China; Shandong Laboratory of Yantai Drug Discovery, Bohai Rim Advanced Research Institute for Drug Discovery, Yantai 264117, P. R. China; University of Chinese Academy of Sciences, Beijing 100049, P. R. China;* orcid.org/0000-0001-7919-9726; Email: xwli@simm.ac.cn

Tao Pang − *State Key Laboratory of Natural Medicines, New Drug Screening and Pharmacodynamics Evaluation Center, China Pharmaceutical University, Nanjing 210009, P. R. China;* orcid.org/0000-0001-5420-2060; Email: tpang@cpu.edu.cn

Yue-Wei Guo − *Shandong Laboratory of Yantai Drug Discovery, Bohai Rim Advanced Research Institute for Drug Discovery, Yantai 264117, P. R. China; School of Medicine, Shanghai University, Shanghai 200444, P. R. China;* orcid.org/0000-0003-0413-2070; Email: ywguo@simm.ac.cn

Authors

Cheng-Long Gao − *State Key Laboratory of Natural Medicines, New Drug Screening and Pharmacodynamics Evaluation Center, China Pharmaceutical University, Nanjing 210009, P. R. China; State Key Laboratory of Chemical Biology, Drug Discovery and Design Center, Shanghai Institute of Materia Medica, Chinese Academy of Sciences, Shanghai 201203, P. R. China; Shandong Laboratory of Yantai Drug Discovery, Bohai Rim Advanced Research Institute for Drug Discovery, Yantai 264117, P. R. China*

Jin-Qian Song − *State Key Laboratory of Natural Medicines, New Drug Screening and Pharmacodynamics Evaluation Center, China Pharmaceutical University, Nanjing 210009, P. R. China*

Ze-Nan Yang − *State Key Laboratory of Chemical Biology, Drug Discovery and Design Center, Shanghai Institute of*

Materia Medica, Chinese Academy of Sciences, Shanghai 201203, P. R. China; Shandong Laboratory of Yantai Drug Discovery, Bohai Rim Advanced Research Institute for Drug Discovery, Yantai 264117, P. R. China; University of Chinese Academy of Sciences, Beijing 100049, P. R. China

Haojie Wang − *Department of Medicinal Chemistry, School of Pharmacy, Fudan University, Shanghai 201203, P. R. China*

Xin-Yuan Wu − *State Key Laboratory of Natural Medicines, New Drug Screening and Pharmacodynamics Evaluation Center, China Pharmaceutical University, Nanjing 210009, P. R. China*

Changwei Shao − *Shandong Laboratory of Yantai Drug Discovery, Bohai Rim Advanced Research Institute for Drug Discovery, Yantai 264117, P. R. China*

Hong-Xia Dai − *Shandong Laboratory of Yantai Drug Discovery, Bohai Rim Advanced Research Institute for Drug Discovery, Yantai 264117, P. R. China*

Kaixian Chen − *State Key Laboratory of Chemical Biology, Drug Discovery and Design Center, Shanghai Institute of Materia Medica, Chinese Academy of Sciences, Shanghai 201203, P. R. China*

Complete contact information is available at: https://pubs.acs.org/10.1021/jacs.4c09695

Author Contributions

[¶]C.-L.G., J.-Q.S. and Z.-N.Y. contributed equally to this work.

Notes

The authors declare no competing financial interest.

■ ACKNOWLEDGMENTS

This work was financially supported by the National Key Research and Development Program of China (2021YFF-0502400, 2022YFC2804100), the National Natural Science Foundation of China (82304373, 42076099, 82174010, 81973512, 81991521), China Postdoctoral Science Foundation funded project (2023M743656), Shandong Laboratory Program (SYS202205), Taishan Scholars Program (tsqn2023-12302), Fundamental Research Projects of Science & Technology Innovation and development Plan in Yantai City (2023JCYJ057), the Open Project of State Key Laboratory of Natural Medicines of China Pharmaceutical University (Grant No. SKLNMKF202405), the Double First-Class Project of China Pharmaceutical University (CPUQNJC22_02), and the CAS Youth Interdisciplinary Team and Shanghai "Super Postdoc" Incentive Program (2022683). Experimental procedures were approved by the Ethical Institutional Animal Care and Use Committee of China Pharmaceutical University, Nanjing, China (2023-06-031). We sincerely thank websites BioRender and SMART for providing some of drawing materials. Dr. Yan Gao and Prof. Xiang-Yang Zhang from Tianjin University are very grateful for the LC-MS/MS analysis of the photoaffinity labeling peptides. We sincerely acknowledge Prof. Guo-Qiang Li from Ocean University of China for the supply of the standard MNP samples to help our structure analysis.

■ REFERENCES

(1) Scott, C. L.; Guilliams, M. Tissue Unit-ed: Lung Cells Team up to Drive Alveolar Macrophage Development. *Cell* **2018**, *175*, 898−900.

(2) Hou, F.; Xiao, K.; Tang, L.; Xie, L. Diversity of Macrophages in Lung Homeostasis and Diseases. *Front. Immunol.* **2021**, *12*, 753940.

(3) Malainou, C.; Abdin, S. M.; Lachmann, N.; Matt, U.; Herold, S. Alveolar macrophages in tissue homeostasis, inflammation, and infection: evolving concepts of therapeutic targeting. *J. Clin. Invest.* **2023**, *133*, No. e170501.

(4) Wang, L.; Wang, D.; Zhang, T.; Ma, Y.; Tong, X.; Fan, H. The role of immunometabolism in macrophage polarization and its impact on acute lung injury/acute respiratory distress syndrome. *Front. Immunol.* **2023**, *14*, 1117548.

(5) Wang, Z.; Wang, Z. The role of macrophages polarization in sepsis-induced acute lung injury. *Front. Immunol.* **2023**, *14*, 1209438.

(6) Zhang, J.; Zhang, M.; Huo, X.-K.; Ning, J.; Yu, Z.-L.; Morisseau, C.; Sun, C.-P.; Hammock, B. D.; Ma, X.-C. Macrophage Inactivation by Small Molecule Wedelolactone via Targeting sEH for the Treatment of LPS-Induced Acute Lung Injury. *ACS Cent. Sci.* **2023**, *9*, 440−456.

(7) Dang, W.; Tao, Y.; Xu, X.; Zhao, H.; Zou, L.; Li, Y. The role of lung macrophages in acute respiratory distress syndrome. *Inflamm. Res.* **2022**, *71*, 1417−1432.

(8) Mehta, P.; Cron, R. Q.; Hartwell, J.; Manson, J. J.; Tattersall, R. S. Silencing the cytokine storm: the use of intravenous anakinra in haemophagocytic lymphohistiocytosis or macrophage activation syndrome. *Lancet Rheumatol.* **2020**, *2*, e358−e367.

(9) Fan, C.; Zhang, Z.; Lai, Z.; Yang, Y.; Li, J.; Liu, L.; Chen, S.; Hu, X.; Zhao, H.; Cui, S. Chemical Evolution and Biological Evaluation of Natural Products for Efficient Therapy of Acute Lung Injury. *Adv. Sci.* **2024**, *11*, No. e2305432.

(10) Behrens, P.; Brinkmann, U.; Wellmann, A. CSE1L/CAS: its role in proliferation and apoptosis. *Apoptosis* **2003**, *8*, 39−44.

(11) Dong, Q.; Li, X.; Wang, C.-Z.; Xu, S.; Yuan, G.; Shao, W.; Liu, B.; Zheng, Y.; Wang, H.; Lei, X.; et al. Roles of the CSE1L-mediated nuclear import pathway in epigenetic silencing. *Proc. Natl. Acad. Sci. U.S.A.* **2018**, *115*, E4013−E4022.

(12) Ngo, L. H.; Bert, A. G.; Dredge, B. K.; Williams, T.; Murphy, V.; Li, W.; Hamilton, W. B.; Carey, K. T.; Toubia, J.; Pillman, K. A.; et al. Nuclear export of circular RNA. *Nature* **2024**, *627*, 212−220.

(13) Huang, J.-L.; Yan, X.-L.; Li, W.; Fan, R.-Z.; Li, S.; Chen, J.; Zhang, Z.; Sang, J.; Gan, L.; Tang, G.-H.; et al. Discovery of Highly Potent Daphnane Diterpenoids Uncovers Importin-β1 as a Druggable Vulnerability in Castration-Resistant Prostate Cancer. *J. Am. Chem. Soc.* **2022**, *144*, 17522−17532.

(14) Yang, Y.; Guo, L.; Chen, L.; Gong, B.; Jia, D.; Sun, Q. Nuclear transport proteins: structure, function, and disease relevance. *Signal Transduct. Target. Ther.* **2023**, *8*, 425.

(15) Zhao, H.; Gong, J.; Li, L.; Zhi, S.; Yang, G.; Li, P.; Li, R.; Li, J. Vitamin E relieves chronic obstructive pulmonary disease by inhibiting COX2-mediated p-STAT3 nuclear translocation through the EGFR/MAPK signaling pathway. *Lab. Invest.* **2022**, *102*, 272−280.

(16) Liang, X.; Luo, D.; Luesch, H. Advances in exploring the therapeutic potential of marine natural products. *Pharmacol. Res.* **2019**, *147*, 104373.

(17) Osgood, C. L.; Chuk, M. K.; Theoret, M. R.; Huang, L.; He, K.; Her, L.; Keegan, P.; Pazdur, R. FDA Approval Summary: Eribulin for Patients with Unresectable or Metastatic Liposarcoma Who Have Received a Prior Anthracycline-Containing Regimen. *Clin. Cancer Res.* **2017**, *23*, 6384−6389.

(18) Barone, A.; Chi, D.-C.; Theoret, M. R.; Chen, H.; He, K.; Kufrin, D.; Helms, W. S.; Subramaniam, S.; Zhao, H.; Patel, A.; et al. FDA Approval Summary: Trabectedin for Unresectable or Metastatic Liposarcoma or Leiomyosarcoma Following an Anthracycline-Containing Regimen. *Clin. Cancer Res.* **2017**, *23*, 7448−7453.

(19) Tang, W.-Z.; Yang, Z.-Z.; Wu, W.; Tang, J.; Sun, F.; Wang, S.-P.; Cheng, C.-W.; Yang, F.; Lin, H.-W. Imidazole Alkaloids and Their Zinc Complexes from the Calcareous Marine Sponge Leucetta chagosensis. *J. Nat. Prod.* **2018**, *81*, 894−900.

(20) Gong, K.-K.; Tang, X.-L.; Liu, Y.-S.; Li, P.-L.; Li, G.-Q. Imidazole Alkaloids from the South China Sea Sponge Pericharax heteroraphis and Their Cytotoxic and Antiviral Activities. *Molecules* **2016**, *21*, 150.

(21) Shi, X.-D.; Zhang, J.-X.; Hu, X.-D.; Zhuang, T.; Lu, N.; Ruan, C.-C. Leonurine Attenuates Obesity-Related Vascular Dysfunction and Inflammation. *Antioxidants* **2022**, *11*, 1338.
(22) Gupta, S.; Khajuria, V.; Wani, A.; Nalli, Y.; Bhagat, A.; Ali, A.; Ahmed, Z. Murrayanine Attenuates Lipopolysaccharide-induced Inflammation and Protects Mice from Sepsis-associated Organ Failure. *Basic Clin. Pharmacol. Toxicol.* **2019**, *124*, 351−359.
(23) Gao, C.-L.; Hou, G.-G.; Liu, J.; Ru, T.; Xu, Y.-Z.; Zhao, S.-Y.; Ye, H.; Zhang, L.-Y.; Chen, K.-X.; Guo, Y.-W.; et al. Synthesis and Target Identification of Benzoxepane Derivatives as Potential Anti-Neuroinflammatory Agents for Ischemic Stroke. *Angew. Chem., Int. Ed.* **2020**, *59*, 2429−2439.
(24) Guo, P.; Li, G.; Liu, Y.; Lu, A.; Wang, Z.; Wang, Q. Naamines and Naamidines as Novel Agents against a Plant Virus and Phytopathogenic Fungi. *Mar. Drugs* **2018**, *16*, 311.
(25) Zhang, N.; Zhang, Z.; Wong, I. L. K.; Wan, S.; Chow, L. M. C.; Jiang, T. 4,5-Di-substituted benzyl-imidazol-2-substituted amines as the structure template for the design and synthesis of reversal agents against P-gp-mediated multidrug resistance breast cancer cells. *Eur. J. Med. Chem.* **2014**, *83*, 74−83.
(26) Tsukamoto, S.; Kawabata, T.; Kato, H.; Ohta, T.; Rotinsulu, H.; Mangindaan, R. E. P.; van Soest, R. W. M.; Ukai, K.; Kobayashi, H.; Namikoshi, M. Naamidines H and I, cytotoxic imidazole alkaloids from the Indonesian marine sponge Leucetta chagosensis. *J. Nat. Prod.* **2007**, *70*, 1658−1660.
(27) Fu, P.-P.; Wang, Q.; Zhang, Q.; Jin, Y.; Liu, J.; Chen, K.-X.; Guo, Y.-W.; Liu, S.-H.; Li, X.-W. Bioactivity-Driven Synthesis of the Marine Natural Product Naamidine J and Its Derivatives as Potential Tumor Immunological Agents by Inhibiting Programmed Death-Ligand 1. *J. Med. Chem.* **2023**, *66*, 5427−5438.
(28) Gibbons, J. B.; Salvant, J. M.; Vaden, R. M.; Kwon, K.-H.; Welm, B. E.; Looper, R. E. Synthesis of Naamidine A and Selective Access to N(2)-Acyl-2-aminoimidazole Analogues. *J. Org. Chem.* **2015**, *80*, 10076−10085.
(29) Jiang, L.; Liu, S.; Jia, X.; Gong, Q.; Wen, X.; Lu, W.; Yang, J.; Wu, X.; Wang, X.; Suo, Y.; et al. ABPP-CoDEL: Activity-Based Proteome Profiling-Guided Discovery of Tyrosine-Targeting Covalent Inhibitors from DNA-Encoded Libraries. *J. Am. Chem. Soc.* **2023**, *145*, 25283−25292.
(30) Castellón, J. O.; Ofori, S.; Burton, N. R.; Julio, A. R.; Turmon, A. C.; Armenta, E.; Sandoval, C.; Boatner, L. M.; Takayoshi, E. E.; Faragalla, M.; et al. Chemoproteomics Identifies State-Dependent and Proteoform-Selective Caspase-2 Inhibitors. *J. Am. Chem. Soc.* **2024**, *146*, 14972−14988.
(31) Li, T.; Wang, A.; Zhang, Y.; Chen, W.; Guo, Y.; Yuan, X.; Liu, Y.; Geng, Y. Chemoproteomic Profiling of Signaling Metabolite Fructose-1,6-Bisphosphate Interacting Proteins in Living Cells. *J. Am. Chem. Soc.* **2024**, *146*, 15155−15166.
(32) Tai, C.-J.; Hsu, C.-H.; Shen, S.-C.; Lee, W.-R.; Jiang, M.-C. Cellular apoptosis susceptibility (CSE1L/CAS) protein in cancer metastasis and chemotherapeutic drug-induced apoptosis. *J. Exp. Clin. Cancer Res.* **2010**, *29*, 110.
(33) Beishline, K.; Azizkhan-Clifford, J. Sp1 and the 'hallmarks of cancer'. *FEBS J.* **2015**, *282*, 224−258.
(34) Kaczynski, J.; Cook, T.; Urrutia, R. Sp1- and Krüppel-like transcription factors. *Genome Biol.* **2003**, *4*, 206.
(35) Wei, L.; Gou, X.; Su, B.; Han, H.; Guo, T.; Liu, L.; Wang, L.; Zhang, L.; Chen, W. Mahuang Decoction Attenuates Airway Inflammation and Remodeling in Asthma via Suppression of the SP1/FGFR3/PI3K/AKT Axis. *Drug Des. Devel. Ther.* **2022**, *16*, 2833−2850.
(36) Pan, H.; Guo, Z.; Lv, P.; Hu, K.; Wu, T.; Lin, Z.; Xue, Y.; Zhang, Y.; Guo, Z. Proline/serine-rich coiled-coil protein 1 inhibits macrophage inflammation and delays atherosclerotic progression by binding to Annexin A2. *Clin. Transl. Med.* **2023**, *13*, No. e1220.
(37) Li, M.; Hu, W.; Wang, R.; Li, Z.; Yu, Y.; Zhuo, Y.; Zhang, Y.; Wang, Z.; Qiu, Y.; Chen, K.; et al. Sp1 S-Sulfhydration Induced by Hydrogen Sulfide Inhibits Inflammation via HDAC6/MyD88/NF-κB Signaling Pathway in Adjuvant-Induced Arthritis. *Antioxidants* **2022**, *11*, 732.
(38) Xu, L.; Hu, W.; Zhang, J.; Qu, J. Knockdown of versican 1 in lung fibroblasts aggravates Lipopolysaccharide-induced acute inflammation through up-regulation of the SP1-Toll-like Receptor 2-NF-κB Axis: a potential barrier to promising Versican-targeted therapy. *Int. Immunopharmacol.* **2023**, *121*, 110406.
(39) Han, H.; Luo, R. H.; Long, X. Y.; Wang, L. Q.; Zhu, Q.; Tang, X. Y.; Zhu, R.; Ma, Y. C.; Zheng, Y. T.; Zou, C. G. Transcriptional regulation of SARS-CoV-2 receptor ACE2 by SP1. *Elife* **2024**, *13*, No. e85985.

https://doi.org/10.1021/jacs.4c09695
J. Am. Chem. Soc. 2024, 146, 28384−28397